Optimization of round-notched specimen for hydrogen embrittlement testing of materials

J. TORIBIO*, F. J. AYASO
Department of Materials Engineering, University of Salamanca, E.P.S., Campus Viriato, Avda. Requejo 33, 49022 Zamora, Spain
E-mail: toribio@usal.es

Many corrosion problems in a wide range of key industries are linked with environmentally assisted cracking (EAC) in its different forms. In fields of activities such as power, chemical and nuclear engineering hydrogen is frequently present as a consequence of electrochemical reactions or hydrogenous working agents. In this framework, the effect of hydrogen environments on the fracture of metals has been well recognized as a significant source of risk of failure, and hydrogen diffusion has been proposed as the key transport mechanism controlling the phenomenon of hydrogen embrittlement (HE).

Slow Strain Rate (SSR) testing is now a well-recognized technique for measuring the susceptibility of metals to environmentally induced fracture, in spite of its inherent limitations regarding strain rate and potential dependence. Development of this method has led to the International Standard *ISO 7539-7* [1] which provides guidelines for this kind of EAC testing. A variety of specimens (initially plain, notched and precracked) can be used (cf. [1]) but the advantages of notched samples in stress corrosion testing have been pointed out, and they are specially recommended for the analysis of hydrogen assisted fracture of metallic materials [2, 3]. Thus the choice of the most appropriate notched specimen is a problem of major technological concern for optimum HE testing in the industry.

In HE processes, hydrogen transportation into prospective microdamage sites in the fracture process zone comprises of several sequential stages: environmental transport to metal, entry into it, and penetration through it. One of the main hydrogen transport mechanisms is lattice diffusion, as discussed elsewhere [4]. Diffusion equations based on both hydrogen concentration and hydrostatic stress distribution were proposed in the past [5, 6]. They consist of the classical Fick's equations modified with a term depending on the hydrostatic stress: hydrogen diffuses not only toward the points of minimum concentration, but also toward those places of maximum hydrostatic stress or, in other words, the sites of maximum hydrostatic strain, where more space is found to be filled by hydrogen. Thus the hydrogen flux density $\mathbf{J}$ depends on the gradients of concentration c and hydrostatic stress $\sigma(\sigma = \operatorname{tr}\boldsymbol{\sigma}/3$, where $\boldsymbol{\sigma}$ is the stress tensor):

$$\mathbf{J} = -D^* \,\mathbf{grad}\, c + Mc\,\mathbf{grad}\,\sigma \tag{1}$$

$$\partial c/\partial t = D^* \Delta c - M\,\mathbf{grad}\, c \cdot \mathbf{grad}\,\sigma - Mc\Delta\sigma \tag{2}$$

where t is the time, D^* the hydrogen diffusion coefficient, and M a second coefficient, a function of the first:

$$M = D * V * /RT \tag{3}$$

where V^* is the molar partial volume of hydrogen, R the ideal gas constant, and T the absolute temperature.

The boundary condition is

$$c_\Gamma = c_0 \exp(V * \sigma/RT) \tag{4}$$

i.e. Boltzmann's distribution where c_0 is the equilibrium concentration without stress. This equation is also the stationary solution of the diffusion problem. The stationary hydrogen concentration is a function only of the hydrostatic stress. In the quasi-static tests (slow enough to neglect time effects) the situation approaches the stationary one.

Thus the question of elucidating the most appropriate notch geometries for HE testing is based on the analysis of hydrostatic stress distributions in the vicinity of the notch tip for each notch geometry, since the hydrostatic stress gradient is relevant to determine the hydrogen diffusion flux according to Equation 1 and the hydrostatic stress at the boundary (notch tip) controls the boundary condition for the diffusion problem according to Equation 4, so that the comparison between different geometries is performed on the basis of their distributions of hydrostatic stress calculated by an elastic-plastic finite element code. The computations allow an analysis of the depth of the maximum hydrostatic stress point (the place towards which hydrogen diffuses) and its evolution with time, and of the two aforesaid key variables, namely the gradient and the boundary value of hydrostatic stress.

This paper studies a wide range of axisymmetric notched specimens in order to choose the most adequate geometry for measuring the hydrogen embrittlement susceptibility of metallic materials in the form of bar or wire, widely used in structural engineering. The numerical modeling, useful for the HE analysis, is based on real experimental results of fracture tests performed on axisymmetric notched samples with very different notch geometries, taken from typical high-strength steel wires for prestressed concrete in civil engineering. The stress–strain curves of the seven steels used in the

*Author to whom all correspondence should be addressed.

0022–2461

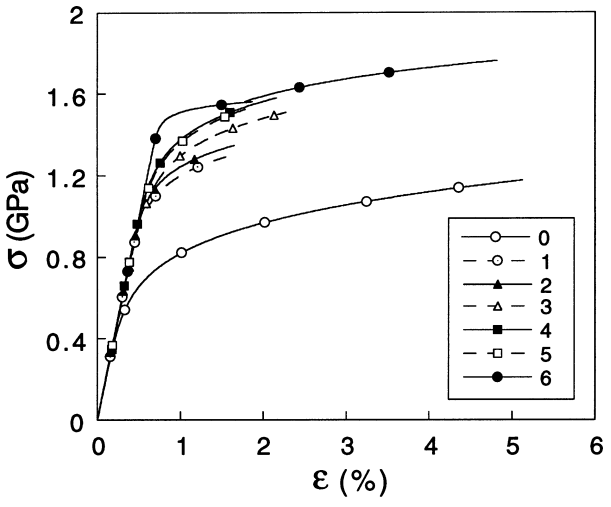

Figure 1 Stress–strain curves of the different steels (from 0 to 6).

computations appear in Fig. 1, and they correspond to different stages of a real cold drawing process to produce prestressing steel wires from a previously hot rolled material. Four notch geometries were used with each material. The dimensions of the specimens were the following:

- Geometry A : $R/D = 0.03$, $C/D = 0.10$
- Geometry B : $R/D = 0.05$, $C/D = 0.30$
- Geometry C : $R/D = 0.40$, $C/D = 0.10$
- Geometry D : $R/D = 0.40$, $C/D = 0.30$

where R is the notch radius, C the notch depth, and D the external diameter of the specimen. These four notched geometries are depicted in Fig. 2.

The finite element method (FEM) with an elastic-plastic code was applied, using a Von Mises yield surface. The external load was applied step by step, in the form of nodal displacements. An improved Newton–Raphson method was adopted, which modified the tangent stiffness matrix at each step. Large strains and large geometry changes were used in the computations by means of an updated Lagrangian formulation to predict the evolution of mechanical variables in the samples after the instant of maximum load (i.e, after the point of instability under load control), up to the instant of final failure by physical separation of the two fracture surfaces (i.e., up to the point of instability under displacement control).

The constitutive equation of the material—as a relationship between equivalent stress and strain—was introduced into the computer program from the real experimental results of the standard tension tests of the considered materials (cf. Fig. 1). The curves were extended for large strains on the basis of the volume conservation in classical plasticity and accounting for the strain hardening evolution to obtain steel 6 from the previous materials (steels 0 to 5). The finite elements used in the computations were isoparametric with second-order interpolation (eight-node quadrilaterals and six-node triangles).

Fig. 3 offers a comparison of one of the load–displacement curves obtained in the fracture experiments and that numerically predicted by using the finite element method (results for steel 0 and geometry D are plotted). It is seen that the agreement is excellent (and the same happens in all cases), which indicates that the numerical modeling is accurate enough to predict the evolution of internal (continuum mechanics variables) in the specimens up to the final fracture moment of instability under displacement control, the numerical prediction of the load decrease part of the curve being also very good.

Figs 4 and 5 show the distributions of hydrostatic stress at the instability point under load control (LC) and at the failure situation or instability point under displacement control (DC) for steels 0 and 6. The hydrostatic stress reaches its maximum at certain distance from the notch tip in geometries A and B (those of minimum notch radius), and at the specimen axis in geometries C and D (those of maximum notch radius). In the latter case of notched specimens C and D there is a displacement of the maximum hydrostatic stress point from the vicinity of the notch tip, during the early stages of the loading process, to the axis of the specimen during the latter stages, including the load decrease part of the load–displacement curve after the

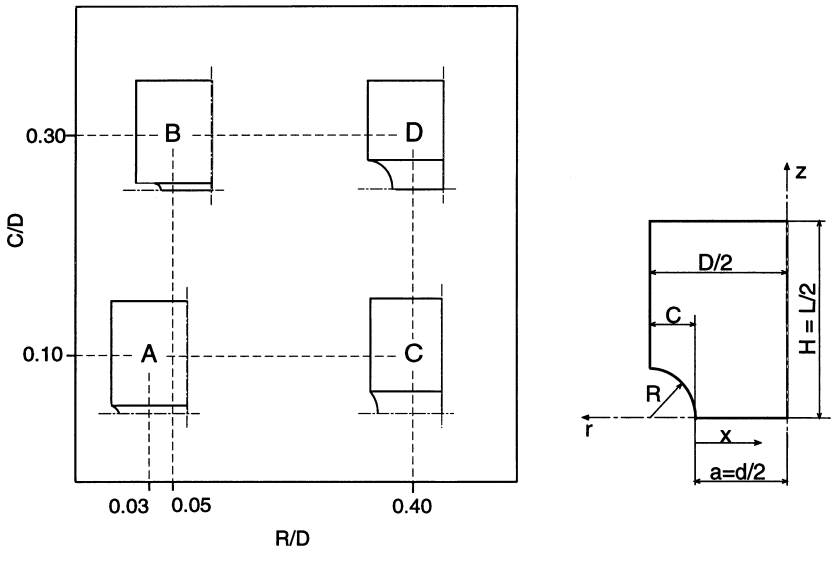

Figure 2 Notched geometries used in the experimental programme.

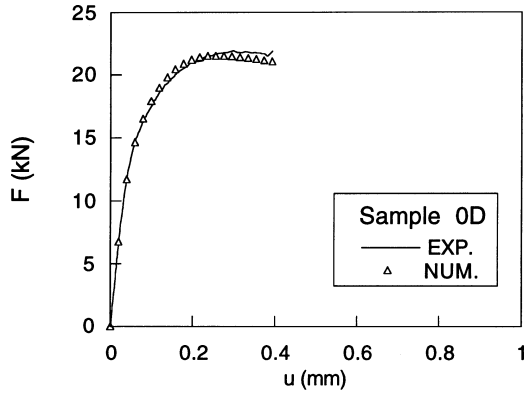

Figure 3 Experimental results (EXP: continuous line) and numerical predictions (NUM: triangles) for steel 0 and geometry D, respectively.

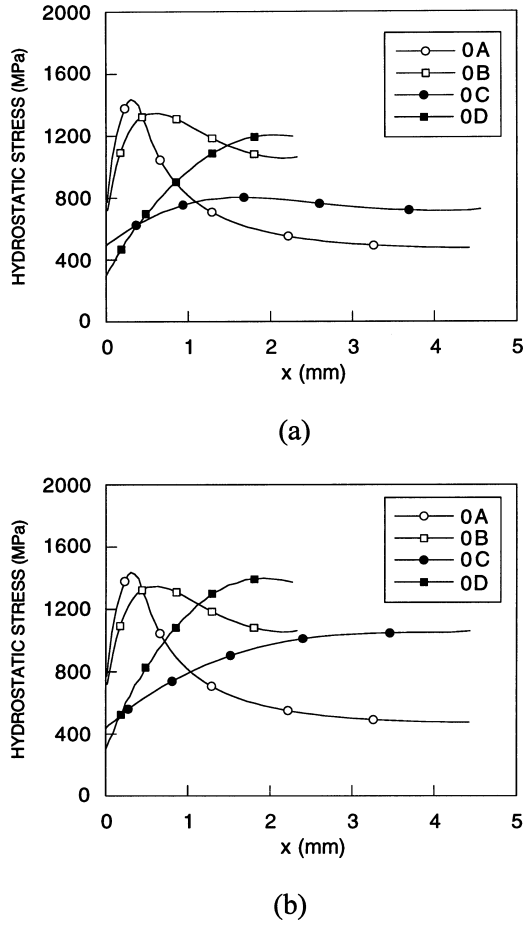

Figure 4 Hydrostatic stress distributions in notched samples A, B, C and D of steel 0, at the instants of LC instability (a) and DC instability (b).

instability point under load control (i.e., the point of maximum load).

The above results demonstrate, firstly, the advantages of notched specimens in HE testing, because they allow the "design" of a certain *hydrostatic stress profile* governing the hydrogen entry and diffusion towards the prospective fracture places. The key items of such a profile are the hydrostatic stress at the notch tip σ_Γ (boundary condition for the hydrogen diffusion problem) and the hydrostatic stress gradient ($d\sigma/dx$).

The hydrostatic stress profiles given in Fig. 5 show no relevant shape differences between steels 0 and 6, i.e., the role of the constitutive equation of the material (given in the plots of Fig. 1) is of minor importance regarding the gradient $d\sigma/dx$, although it is a key parameter in the matter of the magnitude of the hydrostatic stress levels, and particularly of the boundary value σ_Γ which is significantly higher in the high strength steel 6 than in the medium strength steel 0 and thus the former receives more hydrogen ingress than the latter.

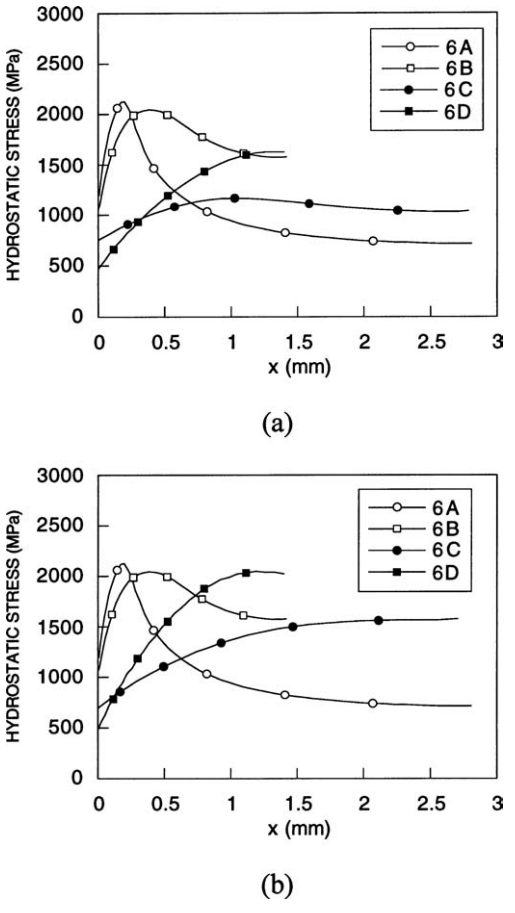

Figure 5 Hydrostatic stress distributions in notched samples A, B, C and D of steel 6, at the instants of LC instability (a) and DC instability (b).

The shape of the hydrostatic stress profile strongly depends on the notch geometry, this being the key finding of the present research. Sharp notch geometries A and B exhibit higher boundary values σ_Γ and higher gradients $d\sigma/dx$ than blunt notch specimens C and D, and therefore the former are more adequate for HE testing than the latter, since they allow a greater hydrogen entry and diffusion towards the critical areas and thus a better evaluation of HE susceptibility of materials. Considering the depth of the maximum hydrostatic stress point, geometry A (shallow notch) is the best to detect surface effects (maximum located near the notch tip), whereas geometry B (deep notch) is the best to analyze the hydrogen penetration toward the inner points.

With regard to the differences between LC and DC instability, they only appear in the case of geometries C and D whose load–displacement plots exhibit load decrease and thus an elevation of hydrostatic stress distributions takes place during the final part of the experiment. However, there is no significant alteration of the hydrostatic stress gradient ($d\sigma/dx$) and the same applies to the boundary value of the hydrostatic stress at the notch tip σ_Γ.

The numerical analysis of the hydrostatic stress distribution in notched geometries demonstrates that sharp notch specimens are the most adequate for hydrogen embrittlement testing, using either shallow notches to detect surface effects or deep notches to analyse hydrogen penetration.

Acknowledgments

The financial support of this work by the Spanish MICYT (Grant MAT2002-01831) and FEDER is gratefully acknowledged.

References

1. ISO 7539-7, Slow strain rate testing (1989).
2. A. W. THOMPSON, *Mater. Sci. Tech.* **1** (1985) 711.
3. J. TORIBIO and M. ELICES, *Corros. Sci.* **33** (1992) 1387.
4. J. TORIBIO, *Mater. Sci. Engng.* **A219** (1996) 180.
5. H. P. VAN LEEUWEN, *Engng. Fracture Mech.* **6** (1974) 141.
6. M. A. ASTIZ, in "Computational Methods for Non Linear Problem", edited by C. Taylor, D. R. J. Owen and E. Hinton (Pineridge Press, Swansea, 1987) p. 271.

Received 5 December 2003
and accepted 6 April 2004